$K^+ + d$ CHARGE-EXCHANGE REACTION FROM 52 TO 456 Mev[*][†]

William Slater, Donald H. Stork, and Harold K. Ticho

Physics Department, University of California, Los Angeles, California

and

Wonyong Lee, William Chinowsky, Gerson Goldhaber, Sulamith Goldhaber, and Thomas O'Halloran

Physics Department and Lawrence Radiation Laboratory, University of California, Berkeley, California

(Received October 23, 1961)

Below the threshold for π-meson production the K^+ meson interacts strongly with nucleons by the following three processes:

Reaction	Scattering amplitude	
$K^+ + p \to K^+ + p$,	$f_1 + f_c$;	(1a)
$K^+ + n \to K^+ + n$,	$\frac{1}{2}(f_1 + f_0)$;	(1b)
$K^+ + n \to K^0 + p$,	$\frac{1}{2}(f_1 - f_0)$.	(1c)

These processes can be described by the Coulomb scattering amplitude f_c and the two charge-independent scattering amplitudes f_0 and f_1, corresponding to the total isotopic spin 0 and 1, respectively.[1]

Elastic $K^+ + p$ scattering experiments give information on the f_1 amplitude. Information on the f_0 amplitude has in the past been obtained from the charge-exchange (CE) scattering of K^+ mesons in complex nuclei.[2,3] These measurements led to determination of total charge-exchange cross sections per neutron, to evidence for p-wave scattering in the $T = 0$ state, and to crude angular distributions of the K^0 mesons.[4] In this work we study the charge-exchange scattering of K^+ mesons on deuterons, in the Lawrence Radiation Laboratory 15-inch bubble chamber filled with deuterium. The chamber was exposed to a highly separated K^+-meson beam,[5] at six different energies: 52, 100, 127, 230, 315, and 456 Mev. For the determination of the charge-exchange cross section we have selected those events giving a subsequent charged decay mode for the K_1^0 meson. This sample corresponds to $\frac{2}{3}$ of all K_1^0 decays and thus to $\frac{1}{3}$ of all charge-exchange events (both K_1^0 and K_2^0 production).[6]

The K^+-meson path length was obtained by two independent methods[7]: (a) by direct measurements of the K^+ tracks in every tenth picture; and (b) by inferring the total path length from the number of "τ-like" decays.[8]

In Table I we list the charge-exchange cross section on deuterium at the six different energies along with the number of events we observed at each energy. In Fig. 1 we show the same cross sections as a function of K^+ kinetic energy in the

Table I. The total $K^+ + d$ charge-exchange (CE) cross sections at various energies and the number of charge-exchange events with subsequent charged K_1^0 decay at each energy.

T (Mev)	Number of CE events	σ_{Kd} for CE (mb)
52 ± 17	13	$1.0^{+0.4}_{-0.3}$
100 ± 13	46	2.7 ± 0.4
127 ± 11	65	3.1 ± 0.4
230 ± 11	161	6.5 ± 0.6
315 ± 6	216	6.7 ± 0.6
456 ± 5	196	6.6 ± 0.7

laboratory system. The scattering angle in the $K^+ n$ c.m. system was calculated by assuming (a) an initially stationary neutron, and (b) a neutron initially moving with a momentum equal and opposite to that of the observed or inferred spectator proton. The momentum of the spectator proton was obtained for each event either by direct observation or by kinematical fitting[9] to the reaction

$$K^+ + d \to K^0 + p + p_{\text{spect}}. \qquad (2)$$

These two different methods gave essentially identical angular distributions. In Figs. 2(a), (b), (c), and (d) we show the observed differential CE cross sections in the laboratory system. In Figs. 2(a'), (b'), (c'), and (d') we show the same data transformed to the $K^+ n$ c.m. system. The curves shown are calculated fits from a phase-shift analysis discussed below in detail.

In order to extract the information on the $K^+ + n$ charge-exchange reaction (1c) from the $K^+ + d$ charge-exchange reaction (2), we use the impulse and closure approximations. The validity of the impulse approximation in this work is examined in two ways[10]: (a) We compare the momentum distribution of the spectator protons with the nucleon momentum distribution in the deuterons as given by the Hulthén wave function. The two are in excellent agreement with each other. (b) We compare the K^0 angle and momentum for each individ-
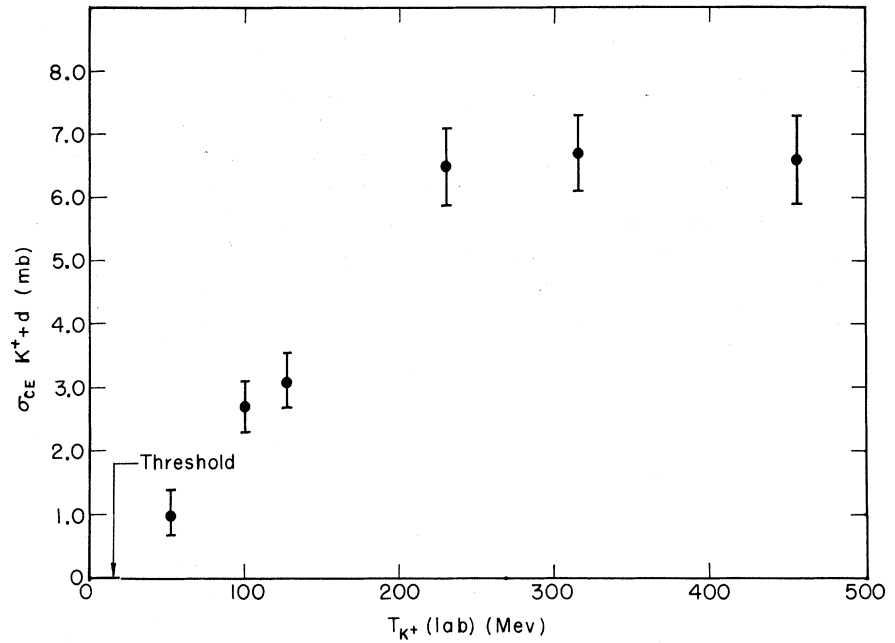
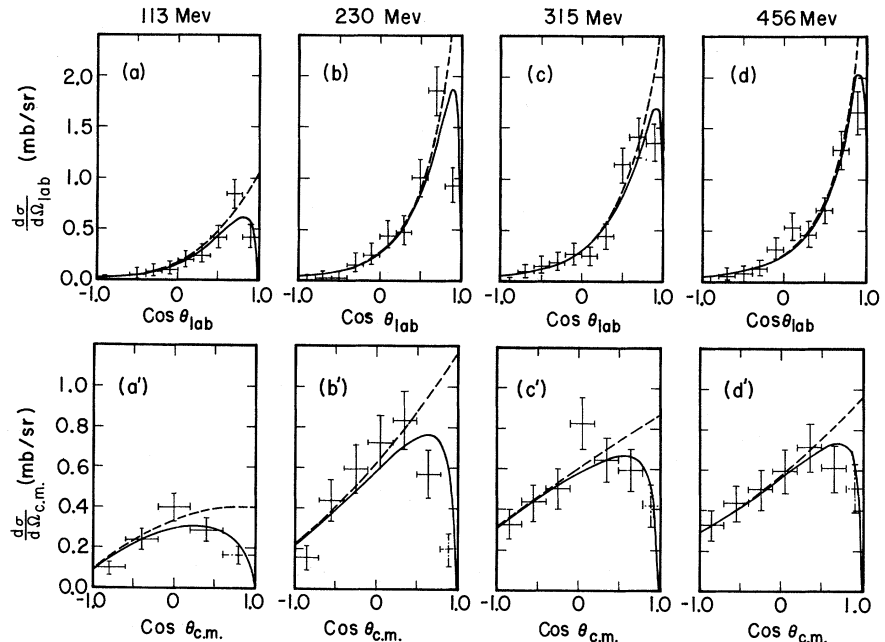FIG. 1. The $K^{+}+d$ charge-exchange cross section as a function of the K^{+} energy.

ual event with the two-body kinematics corresponding to Reaction (1c). With few exceptions, the individual points form a band ± 50 Mev/c around the curve given by the two-body kinematics.

For Reactions (2), the impulse and closure approximations give[11]

$$d\sigma/d\Omega = (1/4k^2)\{[\,|a_1 - a_0|^2 + \tfrac{2}{3}|b_1 - b_0|^2][1 - H_2(\theta)] + \tfrac{1}{3}|b_1 - b_0|^2[1 + H_2(\theta)]\}.$$ (3)

Here all quantities are computed in the c.m. system of a K meson and a stationary neutron,

FIG. 2. The differential K^{+} $+d$ charge-exchange cross sections at a series of K^{+} energies. Figures 2(a), (b), (c), and (d) show the differential cross sections in the laboratory system. Figures 2(a'), (b'), (c'), and (d') show the same cross sections in the c.m. system of K^{+} and an initially moving neutron with momentum equal and opposite to the "spectator" proton. The solid curves were computed from the phase-shift solutions with $T = 1$ s wave and $T = 0$ s and p waves (Solution A, Table II). The dashed curves come from the same solutions, setting $H_2(\theta)$ $\equiv 0$, and thus correspond to the scattering from free neutrons.

$$H_2(\theta) = \frac{2(\alpha+\beta)\alpha\beta}{(\alpha-\beta)^2}\frac{1}{K}\left[\tan^{-1}\left(\frac{K}{2\alpha}\right) - 2\tan^{-1}\left(\frac{K}{\alpha+\beta}\right) + \tan^{-1}\left(\frac{K}{2\beta}\right)\right], \tag{4}$$

where in (4) we approximate K, the momentum transfer in the lab system, by the nonrelativistic value $K \approx 2k\sin(\theta/2)$. This approximation is very good for small values of θ. For large values of θ the function $H_2(\theta)$ is small and insensitive to K. The quantities $\alpha = 45.5$ Mev and $\beta = 7\alpha$ come from use of the Hulthén wave function for the deuteron.

For each isotopic spin we have

$$a_T(\theta) = \sum_{l=0}^{l_{max}}\{(l+1)\eta_{Tl}^{+} + l\eta_{Tl}^{-}\}P_l^0(\theta),$$

$$b_T(\theta) = i\sum_{l=1}^{l_{max}}\{\eta_{Tl}^{+} - \eta_{Tl}^{-}\}P_l^1(\theta).$$

Here $\eta_{Tl}^{\pm}$ refers to $j = l \pm \frac{1}{2}$, and $\hbar k$ is the momentum in the K^+n c.m. system.

In the derivation of Eq. (3) the Pauli principle for the two outgoing protons is taken into account. Correction terms due to the final proton-proton interactions, multiple scattering, and the $K^+ - K^0$ mass difference have not been included. These correction terms are likely to contribute most to small scattering angles. In order to test the importance of these neglected terms we have carried out the phase-shift analysis once for the entire angular interval and once for the angular interval $\cos\theta_{c.m.} < 0.6$. Within the errors, the solutions common to the two cases were the same.

We have carried out a phase-shift analysis[12] for

Table II. Phase-shift solutions with errors. Sets A and B are the small and large s-wave solutions in the sp fit. These phase shifts were computed on the assumptions that (a) the $T = 1$ state can be expressed as a pure repulsive s wave, and (b) $T = 0$ d- and higher angular-momentum waves can be neglected.

T_k (Mev)	Solutions	$T=1$ $S_{1/2}(\delta_1)$ (deg)	$T=0$ $S_{1/2}(\delta_0)$ (deg)	$T=0$ $P_{1/2}(\delta_{01})$ (deg)	$T=0$ $P_{3/2}(\delta_{03})$ (deg)	Probability from χ^2 fit (%)	σ_{Kn}, CE (mb)	σ_{Kn}, elastic (mb)	σ_{Kd}, NCE[a] (mb)	σ_{Kd}, NCE[b] (mb)
					Set A					
113	1	-23	- 6 ± 6	- 7 ± 4	10 ±2	4	4.0 ±0.7	7.9 ±3.1	27	21 ±5
	2			15 ± 4	- 1 ±2					
230	1	-34	13 ± 5	- 4 ± 5	14 ±4	2	8.1 ±0.7	3.8 ±1.0	21	
	2			20 ± 7	2 ±2					
313	1	-41	15 ±10	- 9 ± 7	15 ±7	16	7.5 ±0.5	4.2 ±1.2	20	
	2			23 ±12	- 1 ±2					
456[c]	1	-50	24 ± 4	- 8 ± 3	21 ±3	70	7.5 ±0.4	5.3 ±0.5	19	20 ±2
	2			31 ± 6	2 ±2					
					Set B					
113	1	-23	-33 ± 6	-18 ± 6	4 ±4	20	3.4 ±2.0	24 ±5	47	21 ±5
	2		13 ± 3	-10 ± 4						
230	1	-34	-68 ±12	-26 ±13	15 ±10	50	7.8 ±3.9	29 ±3	45	
	2			29 ±11	-12 ±9					
313	1	-41	-54 ±20	-57 ±15	10 ±8	20	7.3 ±2.7	26 ±5	40	
	2			48 ±15	-19 ±8					
456	1	-50	-76 ±12	-75 ±30	2 ±10	70	6.9 ±1.9	23 ±2	35	20 ±2
	2			59 ±30	-20 ±10					

[a]σ_{Kd}, NCE, the $K + d$ non-charge-exchange cross section, is calculated with a cutoff angle of $\cos\theta_{lab} = 0.94$. Errors in the calculated σ_{Kd}, NCE reflected from errors in phase shifts are ≤ 3 mb and are not quoted.

[b]The value at $T_K = 456$ Mev comes from reference 16. The value quoted at 113 Mev was obtained from our own data[12] at 100 Mev.

[c]An additional large positive $T = 0$ s-wave solution exists for this energy with σ_{Kn}, elastic ≈ 12 mb, namely: $\delta_0' = 55°$, and $(\delta_{01}', \delta_{03}') = (-9°, +20°)$ or $(+25°, -3.5°)$. Here δ_{01}' and δ_{03}' have the same values (within the errors) as in solutions A_1 and A_2 for 456 Mev above, while δ_0' is related to δ_0 through $|\delta_1 - \delta_0'| \approx \pi - |\delta_1 - \delta_0|$. The ambiguity observed here always occurs for $|\delta_1 - \delta_0| \approx \pi/2$.

the differential cross sections at kinetic energies 113, 230, 315, and 456 Mev. Each energy was treated independently. In our analysis the $T = 1$ phase shifts were assumed to be pure s-wave phase shifts[13] and were taken from the $K^+ + p$ data.[14,15] We solved for the $T = 0$ phase shifts assuming the scattering process in the $T = 0$ state to be (a) s- and p-wave, and (b) s-, p-, and d-wave.

(a) Permitting the scattering to occur in the $T = 0$ s and p states leads to two sets of solutions, A and B, each with its Fermi-Yang ambiguity (see Table II). The two solutions A and B differ principally in the sign and magnitude of the $T = 0$ s wave. Solutions A and B lead to $K^+ + n$ cross sections which differ from each other by a factor of about four, and $K^+ + d$ non-charge-exchange (NCE) cross sections which differ by a factor of about two. Experimentally we know the total $K^+ + d$ cross sections at two of the energies,[16] and from these obtain values for the $K^+ + d$ NCE cross sections. The values obtained from solution A are in good agreement with those obtained from experiment. Solution B, which gives a better χ^2 fit to the differential CE cross section, can be definitely ruled out because it leads to too large a $K^+ + d$ NCE cross section. We are thus left at each energy with the two Fermi-Yang solution sets A_1 and A_2. The solid curves in Fig. 2 present the differential CE cross section computed from solutions A both in the laboratory and in the center-of-mass systems. The dashed curves were computed from the same phase shifts by setting $H_2(\theta) \equiv 0$ in Eq. (3). The difference between the dashed and solid curves thus illustrates the suppression of the forward scattering due to the Pauli exclusion principle. In Fig. 3 we show the energy dependence of the phase shifts obtained in solutions A_1 and A_2. It is interesting to note that in contrast to the $T = 1$ s-wave phase shifts, which are negative (repulsive potential), the $T = 0$ s-wave phase shifts are positive (attractive) over the energy interval from about 150 to 456 Mev. From the present data we cannot conclude, however, whether at lower energies δ_0 would remain attractive or turn weakly repulsive.

(b) In an attempt to improve the goodness of fit to our data, we have introduced two more parameters in our phase-shift analysis corresponding to $d_{3/2}$ and $d_{5/2}$ waves.[12] The introduction of these two additional parameters improves the fit somewhat but, as expected from our limited statistics, increases the uncertainty on all values of the phase shifts. The solutions obtained can be divided into three sets, of which two are similar to sets A and
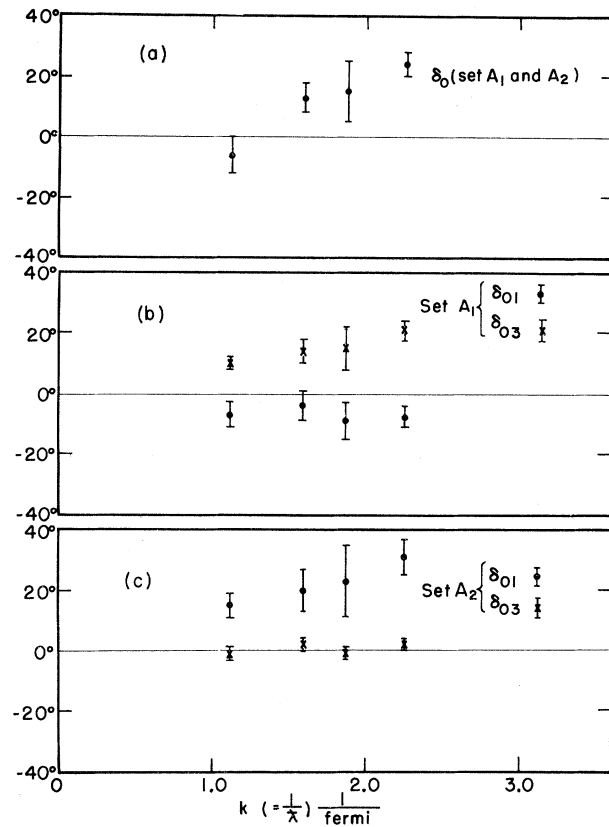

FIG. 3. The phase-shift solution sets A_1 and A_2 (see Table II) as a function of k, the momentum in the $K^+ n$ c.m. system, expressed in inverse fermis (10^{13} cm^{-1}). Not shown in the figure is one further ambiguity in δ_0 at 456 Mev, giving $\delta_0 = 55$ deg. (See Table II, footnote c.)

B with small d-wave phase shifts added. Here again we can rule out the solution similar to B on comparison with the experimental NCE σ_{Kd}. The third set of solutions tries to fit the data with small negative δ_0 phases, from -5 deg to -15 deg, small p-wave phases, and d-wave phase shifts of which one ranges from -15 deg to -30 deg and the other is small and positive. We must stress, however, that the statistics of our data permit us only to make a first exploration into the domain of higher partial waves which may contribute to the scattering process.

experiment would not have been possible. We would also like to acknowledge the important contributions of Theodore Stubbs and Jean Fisk, as well as helpful discussions with Professor K. M. Watson.

*Work submitted in part to the University of California by Wonyong Lee in partial fulfillment of the requirements for the Ph.D. degree.

†This work was done under the auspices of the U. S. Atomic Energy Commission.

[1]In this analysis we consider the K^+ and K^0 mesons to form an isotopic-spin doublet. In this connection, see A. Pais [Phys. Rev. 112, 624 (1958)], who discusses the consequences of K-meson singlets with opposite parity.

[2]M. A. Melkanoff, O. R. Price, D. H. Stork, and H. K. Ticho, Phys. Rev. 113, 1303 (1959); B. Secchi-Zorn and G. T. Zorn, Phys. Rev. 130, 1898 (1960); D. Keefe, A. Kernan, A. Montwill, M. Grilli, L. Guerriero, and G. A. Salandin, Nuovo cimento 12, 241 (1959).

[3]M. N. Whitehead, R. E. Lanou, V. Cook, Jr., and R. W. Birge, Phys. Rev. 118, 300 (1960).

[4]E. Helmy, D. J. Prowse, and D. H. Stork, Nuovo cimento 19, 179 (1961).

[5]G. Goldhaber, S. Goldhaber, T. Kadyk, T. Stubbs, D. H. Stork, and H. K. Ticho, Lawrence Radiation Laboratory Internal Report Bev-483, 1960 (unpublished).

[6]See, for example, F. Crawford, Jr., M. Cresti, R. Douglass, M. Good, G. Kalbfleisch, M. Stevenson, and H. Ticho, Phys. Rev. Letters 2, 266 (1959).

[7]At 52 Mev, Method (a) only was used. At 456 Mev, Method (b) only was used.

[8]By "τ-like" decays we mean K^+ decays into three charged secondaries; these correspond to a fraction $f_1 = 0.061 \pm 0.002$ of all K^+ decays. This number is a weighted average of results quoted by L. B. Okun, Ann. Rev. Nuclear Sci. 9, 61 (1959), and our own measurements on stopping K^+ mesons. In both cases the branching ratio obtained for these decay modes was $f_1 = 0.061 \pm 0.003$.

[9]The spectator proton was identified by comparing the fitted quantities of both protons with a track computed on the assumption of K^+ scattering off a neutron.

We found the lower momentum proton to fulfill the properties of the spectator in nearly all of the events, and utilized this method for the selection of the spectator (reference 10). In this work we utilized the geometrical reconstruction (PANG) and kinematical fitting (KICK) programs of the Alvarez Group. J. P. Berge, F. T. Solmitz, and H. D. Taft, Rev. Sci. Instr. (to be published), and A. H. Rosenfeld and J. M. Snyder, Rev. Sci. Instr. (to be published).

[10]The graphs showing these distributions were presented at the 1960 Rochester Conference [W. Chinowsky, G. Goldhaber, S. Goldhaber, W. Lee, T. O'Halloran, T. Stubbs, W. Slater, D. H. Stork, and H. K. Ticho, in Proceedings of the 1960 Annual International Conference on High-Energy Physics at Rochester (Interscience Publishers, Inc., New York, 1960), p. 451.

[11]S. Fernbach, T. Green, and K. Watson, Phys. Rev. 84, 1084 (1951); R. Rockmore, Phys. Rev. 105, 256 (1957); K. Rogers and L. Lederman, Phys. Rev. 105, 247 (1957); E. Ferreira, Phys. Rev. 115, 1727 (1959); and M. Gourdin and A. Martin, Nuovo cimento 11, 670 (1959); 14, 722 (1959).

[12]For details see Wonyong Lee, thesis, Lawrence Radiation Laboratory Report UCRL-9691, 1961 (unpublished).

[13]We have also explored the behavior of the $T = 0$ phase shifts for the case of p waves in the $T = 1$ state. For dominant $T = 1$ $p_{1/2}$ solutions (reference 14) we obtain $T = 0$ solutions which can be identified with the Minami transformations of solutions A and B quoted in Table II. For the $T = 1$ $p_{1/2}$ and $p_{3/2}$ dominant solutions (reference 14) we obtain several solutions by fitting the differential charge-exchange cross section, most of which can be ruled out on comparison with the experimental σ_{Kd}, NCE. At present the evidence for dominant p-wave scattering in the $T = 1$ state is not strong enough to warrant a thorough study of solutions other than those containing pure s wave in the $T = 1$ state.

[14]T. Stubbs, H. Bradner, W. Chinowsky, G. Goldhaber, S. Goldhaber, W. Slater, D. H. Stork, and H. K. Ticho, Phys. Rev. Letters 7, 188 (1961).

[15]T. F. Kycia, L. T. Kerth, and R. G. Baender, Phys. Rev. 118, 553 (1960).

[16]V. Cook, D. Keefe, L. T. Kerth, P. G. Murphy, W. A. Wenzel, and T. F. Zipf, Phys. Rev. Letters 7, 182 (1961). See also footnote in Table II.